Chaboche Model for Fatigue by Ratcheting Phenomena of Austenitic Stainless Steel under Biaxial Sinusoidal Loading

Fatiha Boussalih [1*], Kamel Fedaoui [1], Tahar Zarza [2]

[1] Institute of Applied Sciences and Techniques - ISTA, Constantine 1 University, Constantine, Algeria.

[2] Civil Engineering Laboratory, Constantine 1 University, Constantine, Algeria.

Abstract

This study deals with the investigation of the cyclic behaviour of 316L and 304L austenitic stainless steels in oligocyclic fatigue under biaxial loading. As a first step, we investigated the prediction of the character of 316L steel under imposed stress, by the fixation of a stress and the evolution of another, forming a cross-proportional loading path in a range of stresses. In addition, the analysis of the behavior of steel 304L with respect to the bi-axial union (primary and secondary loadings) was studied in order to produce the ratcheting phenomenon induced by the non-zero mean stress, governing the structure to damage in two opposite directions, diagonally symmetrical. An appreciable confrontation of the intrinsic characters of the two steels under the same loading conditions was discussed in the last intervention, controlled in strain, generating the phenomenon of cross-hardening and imposed stress. Producing the progressive strain that manifests itself at each loading cycle will make it possible to quantify the degree of plasticity of each material and optimize the most relevant steel. In this numerical study, the Chaboche model is selected, which is based mainly on perfect predictions and robust constitutive laws capable of reproducing observed macroscopic phenomena. All the simulations were carried out using the ZéBulon computation code. A lot of work on the behavior of 304L and 316L stainless steel has been carried out by several researchers in recent years. The results of previous experiments and numerical simulations have been compared to the results of this study, and a good match has been found.

Keywords: 316L SS; 304L SS; Sinusoidal Fatigue; Ratcheting; Plastic; Chaboche Model.

1. Introduction

Multiaxially loaded oligocyclic fatigue is encountered in many structures and can result in the failure of material and structures. Numerical modeling techniques must then take into consideration the complexity of the material, mechanisms, and phenomena observed by an adequate model. The modeling of the behavior of austenitic stainless steels is still an open subject, despite the diversity of models or criteria existing in this field. The complexity is mainly based on the penalizing interaction of different stresses (mechanical, thermal, or chemical), the dispersions on the properties of the material, the ignorance of the geometry and of the loadings, the randomness of the material, the plastic deformations Cyclic cycles generated by the repetition of stresses, even below the elastic limit of the material, play a major role in oligocyclic fatigue and can lead to the failure of parts in service [1, 2]. All these factors increase the difficulty of modeling [3, 4]. Uniaxial tests are inexpensive, easy to perform, and provide useful information about material behavior [5, 6]. Even so, most parts in service are subject to complicated loads and aren't properly checked and tested [7].

---

* Corresponding author: bornifatiha@yahoo.fr

The study of the behavior of a material is a process of observing, describing, and analyzing the phenomena involved and obtaining numerical answers. This last approach is exploited in order to draw cyclic curves, giving rise to different phenomena: hardening, softening, accommodation, adaptation, and ratcheting [8-10]. This last phenomenon has been widely studied by Taleb et al. (2006) [11], Hassan et al. (2008) [12], Taleb et al. (2009) [13], Taleb et al. (2011) [14], Halama et al. (2012) [15], Meggiolaro et al. (2015, 2016) [16, 17]. The sensitivity and foresight of the comportment of the 304L steel have been an numerical field of investigation led by Boussalih et al. (2019) [18]. In addition to some experimental investigations and simulations, the work of Belattar and Taleb (2021) [19], was carried out on both 304L and 316L steels, the results made it possible to predict several cyclic phenomena, under imposed stress and strain, under cross loading, experimentally and numerically using the Multi-Mechanism (MM) model.

In this study, the behavior of the two steels, 304L and 316L, under biaxial alternating loading (traction-torsion) will be predicted. By opting for the model of Chaboche, we then diagnose their phenomenological and macroscopic behavior. Biaxial fatigue is encountered in the oil and gas industries, in energy installations, and in the chemical industries [19, 20]. It was a motivating subject for several researchers [21–23]. Other researchers look into biaxial fatigue in [24–28]. The notoriety of austenitic stainless steels is based primarily on their excellent mechanical attributes such as ductility, impact resistance, and toughness [29-36]. This study aims to simulate and correctly predict the nonlinear behavior of the two 316L and 304L steels. The industrial inventory brings into play macroscopic phenomena such as: elastic shakedown, plastic shakedown, ratcheting, softening, hardening, creep, all related to the plasticity of the material, which leads to the damage of structural components subjected to a wide variety of stresses of mechanical origin. The cyclical nature of this behavior threatens the safety of structures and is induced by the phenomenon of fatigue, which appears as a consequence of this formalism.

The prediction of the discrete character of the two steels studied requires the control of their behavior based primarily on the understanding of the macroscopic phenomenological observations during cyclic plasticity, allowing for numerical simulations by the application of the sinusoidal bi-axial stresses in oligocyclic fatigue, which depends only on the number of cycles and not on the frequency. It is driven by two decisive factors: cyclic stress and strain, and proliferating plasticity, which progresses and subsequently produces damage. The ratcheting phenomenon represents the progressive strain which leads to sudden and catastrophic failure caused by the non-zero mean stress propagating rapidly in the structure. This subject will be discussed further in this study.

The first step explores a discussion between the two interacting loading scenarios in order to identify the predictive ratchet at failure by the application of bi-axial tensile-compression stresses followed by a non-zero stress torsional loading applied to 316L steel, by opting for the Chaboche model using the Zebulon calculation code. The second part of this work is concerned with the prediction of the elastoplastic character of steel 304L under an associated proportional cyclic stress field, generating a biaxial ratcheting phenomenon, diagonally symmetrical, shown by the evolution of the stress as a function of deformation. The last part is devoted to the comparison of the two steels 304L and 316L, showing the phenomenon of over hardening called "cross-hardening effect", induced by the application of the loading: primary in the axial direction, followed by a secondary loading in the direction of torsion at imposed strain shown by hysteresis loops. An estimate of the fastest ratcheting between the two steels studied, which led to failure, generated almost the same level of stress over several successive cycles and was studied. In the conclusion section, a summary of the results will be provided along with recommendations for future studies.

2. Methodology

A better description of the macroscopic behavior of the material requires the choice of an appropriate model and the implementation of the various steps, and should follow the steps in the process:

- The choice of model (Chaboche Model).

- The model chosen uses material parameters corresponding to the two steels studied, resulting from the literature (Table 2).

- A validation on the first hysteresis loops of the uni-axial tension-compression tests, in order to ensure the adequate choice of the model chosen and its capacity to suitably describe the elastoplastic behavior (Figures 1 and 2).

- The concordance between the results of the numerical simulation and the experimental data allows the performance of various simulations on steels.

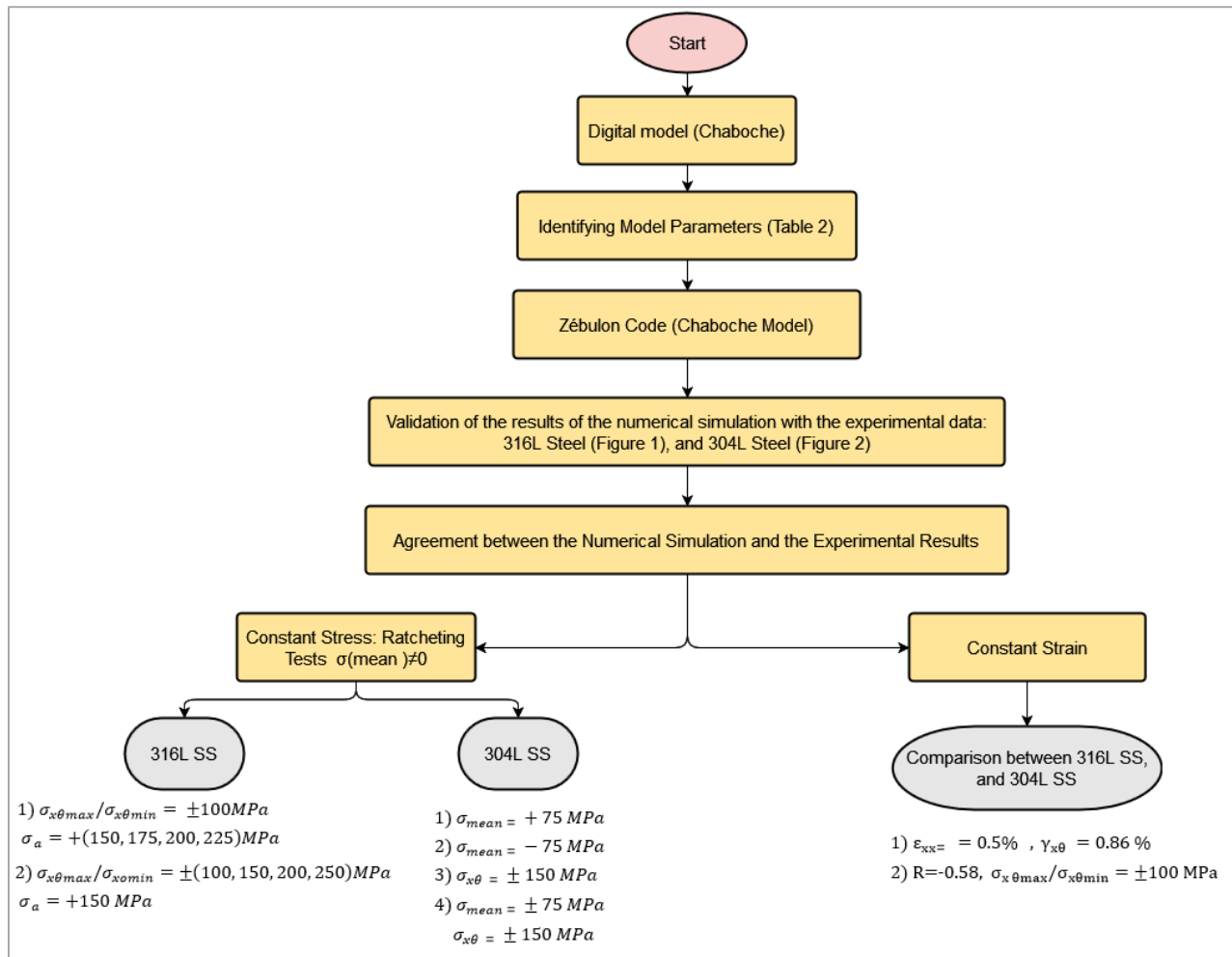This strategy requires a complete hierarchy, which is shown in the flowchart of Figure 1.

Figure 1. Modeling strategy of elastoplastic behavior

3. Chaboche Material Model

The Chaboche formulation was presented for the cyclic behavior of metals using nonlinear hardening models. The Chaboche material model can handle tension-compression cyclic loadings where the hardening properties change. Depending on what type of material, temperature, or initial states are used, the material may soften or harden. The field of pure reversibility is delimited in the space of the stresses by a surface of load described by von Mises from which plastic flow can occur [15, 37]. This surface is represented in the constraint space by a load function of the following form:

$$f = J\,(\sigma - X) - R - \sigma_{yi} \tag{1}$$

where, J is the second invariant of the deviatoric tensor of the stress. The material studied is characterized by its resistance to rupture and its ability to work hard. Consequently the work hardening is manifested by the expansion of the load surface corresponds to an isotropic work hardening (R) and the displacement of its center corresponds to a kinematic work hardening (X). The evolution of R is given by:

$$dR = b\,(Q - R)dp \tag{2}$$

where, Q and b are constants of the material which have the effect of introducing a progressive hardening or softening. The evolution of kinematic hardening (X) is given by:

$$d\underline{X} = \tfrac{2}{3}C(p)d\underline{\varepsilon}^p - \gamma(p)\,\underline{X}dp \tag{3}$$

where, C and γ being characteristic coefficients of each material, dp is the increment of the cumulated plastic deformation:

$$dp = \left[\frac{2}{3} \, d \, \underline{\varepsilon}^p : \underline{\varepsilon}^p \right]^{1/2} \tag{4}$$

The evolution of the kinematic hardening variable (X) is given by the model proposed initially by Armstrong and Frederick (1966) introducing a recall term, called dynamic recovery:

$$\dot{X} = 2/3 \, C \, \dot{\varepsilon}^{\cdot P} - \gamma X \dot{p} \tag{5}$$

4. Verification of the Model

The Chaboche model adopted in this study is based on the association of two nonlinear isotropic and kinematic hardening, in order to describe the behaviour of 316L and 304L stainless steel alloys, the chemical composition and mechanical properties of these material are presented in Tables 1, and 2. The parameters of the Chaboche model used in this study are those obtained from the works of Flavien et al. (2012) [25] for 316L and Djimli et al. (2010) [38], which will be implemented in the Zebulon calculation code [39], see Table 2.

Table 1. Chemical composition of 316 L SS and 304L SS [19]

316 L	C	Si	Mn	Ni	Cr	Mo	P	S
	0.02	0.36	1.32	10.13	16.57	2.03	0.04	0.029
304 L	C	Si	Mn	Ni	Cr	N	P	S
	0.028	0.68	1.54	9.04	18.83	0.085	0.035	0.026

Table 2. Mechanical properties and parameters of Chaboche model for 316L and 304L SS

	E (GPa)	ν (-)	σ_y (MPa)	Q (MPa)	b	C (MPa)	γ
316L	190	0.3	110	90	0.3	112.500	580
304L	206	0.3	160	45	35	51200	500

The first step before starting the simulation, it is necessary to carry out the comparison between the first hysteresis loops of the simulation and experimental cyclic curve, carried out between ± 0.5% at deformation imposed with a tensile-compression cycle, in order to ensure the reliability of the parameters materials chosen before their use.

Figure 2-a shows the comparison between the simulation curve, performed by the computer code ABAQUS and the experimental test on 316L steel, by cyclic loading carried out by Roya et al. [40]. On the other hand, the simulation of the present study is carried out by the finite element calculator code ZéBulon (Figure 2-b). Figure 3-a is a cyclic confrontation curve, between simulation calculated by the ZéBulon code relating to 304L steel, led by Bouusalih et al. [18]. In the present study, we see that there is a good agreement between simulation and experiment (Figure 3-b).
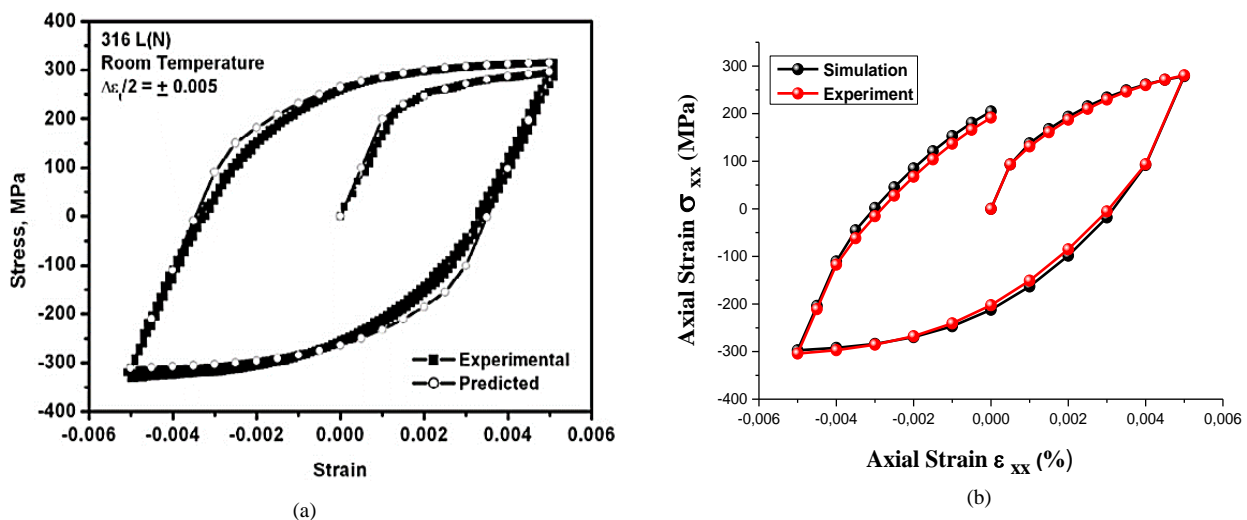

(a)

(b)

Figure 2. Comparison of first cycle hysteresis loop obtained from experiment and simulation, ± 0.5 % strain amplitude for 316L SS; a) Comparison of cyclic behavior Roy et al. (2013) [40]; b) superposition of cyclic behavior in the present study.
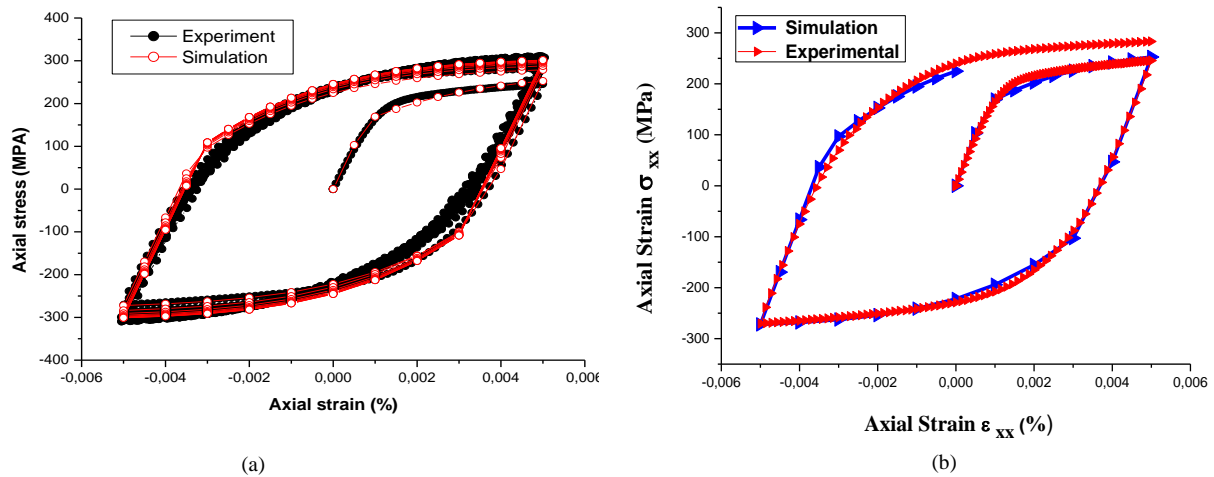
(a)

(b)

Figure 3. Comparison of first cycle hysteresis loop obtained from experiment and simulation, ± 0.5 % strain amplitude for 304L SS, a) Comparison of cyclic behavior Boussalih et al. (2019) [18], b) superposition of cyclic behavior in the present study.

5. Results and Discussion

5.1. Ratcheting Experiments on Stainless Steel 316L

In order to predict the cyclic behavior of 316L steel pipe under biaxial cyclic loading performed by Moslemi et al. [41], using the finite element calculation code ANSYS (Figure 4-a). The Chaboche model has been exploited for its ability to correctly simulate the different plastic deformation curves obtained as a function of the number of cycles, and compared with the experimental test (Figure 4-b) uniaxial ratcheting with non-zero mean stress occupied a key place, in this study shown by the evolution hysteresis loops (Figure 4-c).
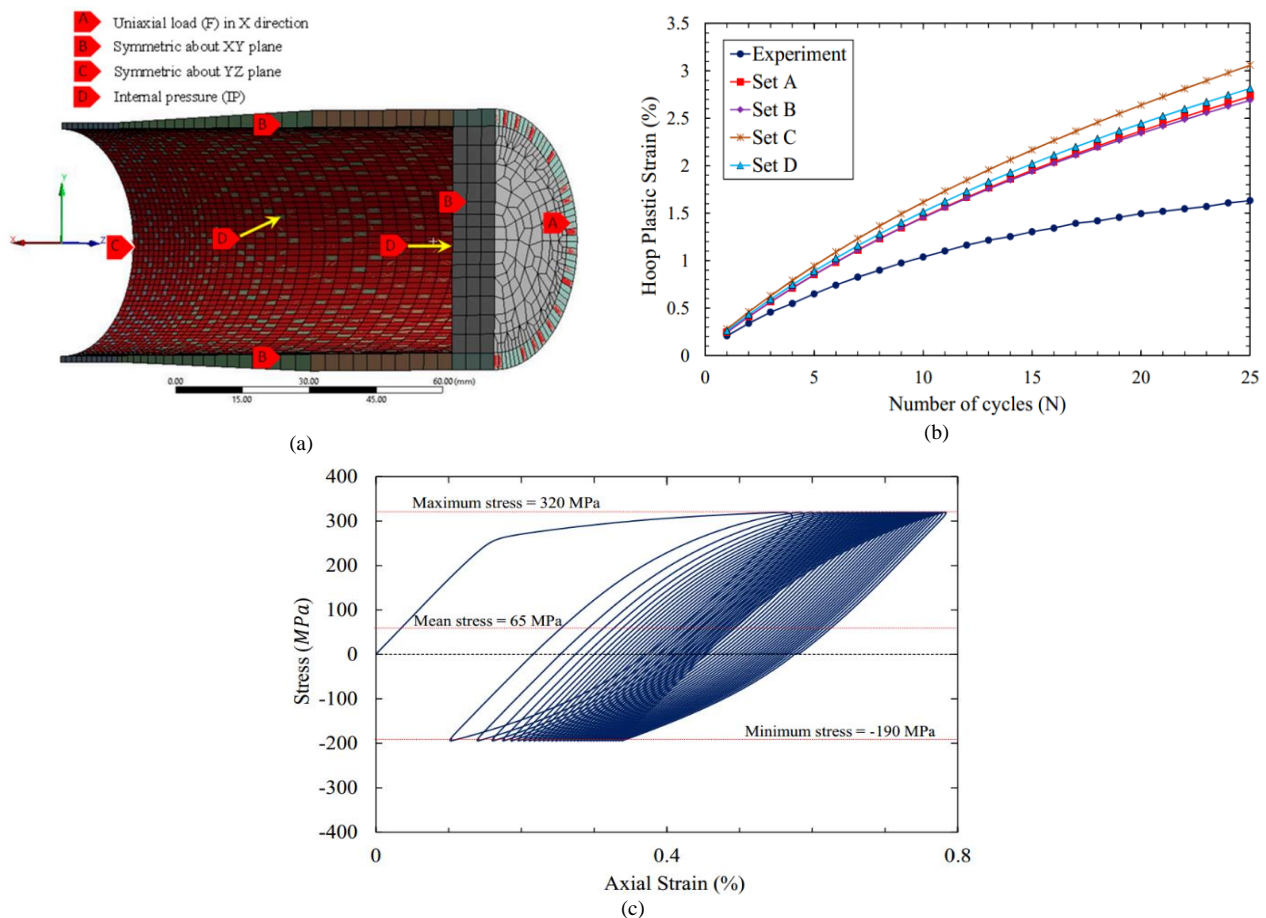

(a)

(b)

(c)

Figure 4. Experimental test on 316L SS steel, a) finite element model of biaxial specimen b) biaxial ratcheting rate, c) Uniaxial ratcheting, Moslemi et al. (2019) [41]

5.2. Numerical Simulation under Bidirectional Sinusoidal Stress

Impact of Increasing Tensile Loading at Constant Torsion

In order to perceive the influence of the tension loading on the work hardening, we carried out four simulations on the steel 316L with increasing amplitude stress and a loading in constant torsion. The loading conditions are shown in the Table 3.

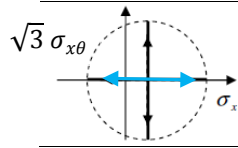**Table 3. Biaxial alternative loading conditions**

		Loading 1	Loading 2	Loading 3	Loading 4
σ_{max}	(MPa)	+ 250	+ 250	+ 250	+ 250
σ_{min}	(MPa)	- 50	- 100	- 150	- 200
$\sigma_{mean=\frac{\sigma_{max}+\sigma_{min}}{2}}$	(MPa)	+ 100	+ 75	+ 50	+ 25
$\sigma_{a=\frac{\sigma_{max}-\sigma_{min}}{2}}$	(MPa)	+ 150	+175	+ 200	+ 225
$\sigma_{x\theta max}/\sigma_{x\theta\,min}$	(MPa)	± 100	± 100	± 100	± 100

Figure 5 shows stress-strain hysteresis curves, revealing a decreasing hardening proportional, when the loading in torsion is constant. The curves obtained, see Figure 6 translate the plastic deformation peaks, resulting in an apparent progressive ratcheting rate, as a function of the number of cycles.
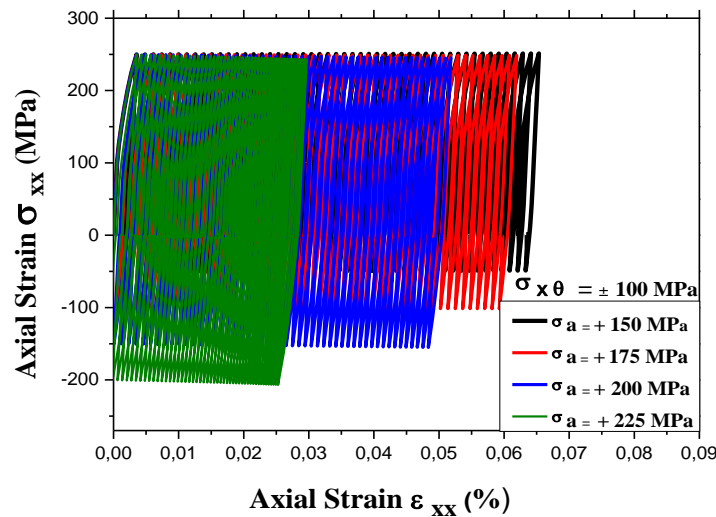

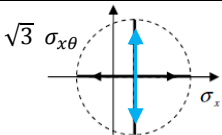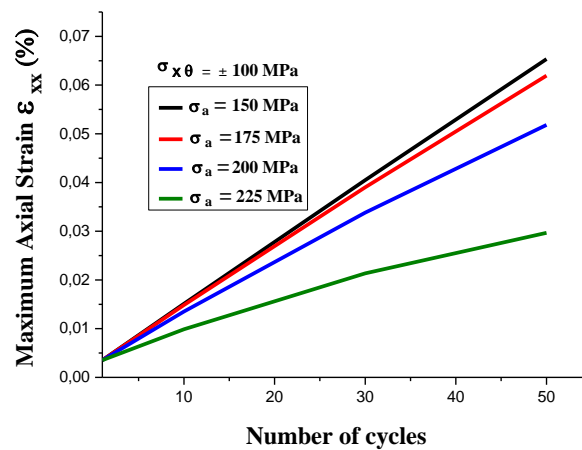**Figure 5. Evolution of the ratcheting rate under biaxial load at different stresses amplitudes**

Figure 6. Axial strain peaks versus the number of cycles under biaxial load at different stresses amplitudes for constant torsion of 316L

Impact of Increasing Torsional Loading at Constant Tension

The present simulation was carried out with a reverse approach to the previous test. Four simulations were performed on 316L steel at constant stress amplitude with increasing torsional load. The loading conditions are shown in Table 4.

Table 4. Biaxial sinusoidal loading conditions

		Loading 1	Loading 2	Loading 3	Loading 4
σ_{max}	(MPa)	+ 200	+ 200	+ 200	+ 200
σ_{min}	(MPa)	- 100	- 100	- 100	- 100
$\sigma_{mean=\frac{\sigma_{max}+\sigma_{min}}{2}}$	(MPa)	+ 50	+ 50	+ 50	+ 50
$\sigma_{a=\frac{\sigma_{max}-\sigma_{min}}{2}}$	(MPa)	+ 150	+ 150	+150	+150
$\sigma_{x\theta max}/\sigma_{x\theta\ min}$	(MPa)	± 100	± 150	± 200	± 250

The phenomenological analysis of the behaviour of the two alloys in cyclic loading (Figure 7), shows stress-strain hysteresis curves describing the fatigue of steel by the ratcheting phenomenon under various loading cases. One observes in particular a ratcheting growing in the opposite direction of the intensity of the loading in torsion. The curves obtained (Figure 8) the plastic deformation peaks resulting in an apparent progressive ratcheting rate as a function of the number of cycles.
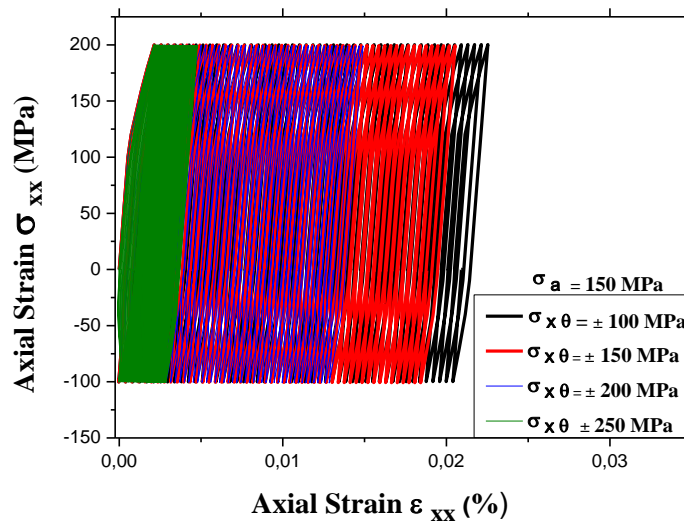

Figure 7. Evolution of the ratcheting rate in biaxial loading at different torsional stresses for stress amplitude constant of 316L
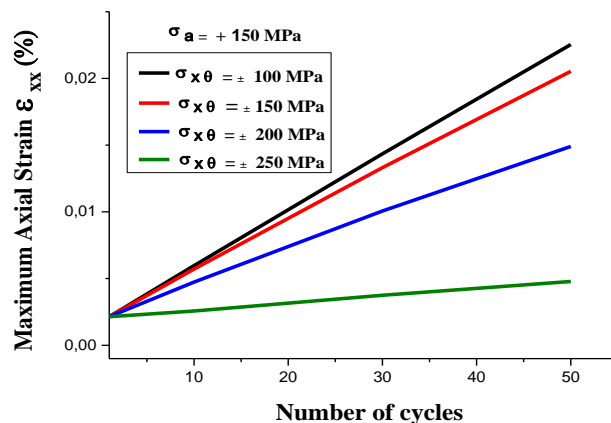

Figure 8. Axial strain peaks versus the number of cycles in biaxial loading at different torsional stresses for stress amplitude constant of 316L

5.3. Investigations of the Ratcheting Phenomena of 304L SS

Ratcheting Experiments on Stainless Steel 304L

According to the experiments carried out on the behavior of 304L steel by Hassan Tasnim &al, under stress cyclic, of average stress σ_{xm}= 50 MPa in the uniaxial direction (Figure 9-a), and an equivalent stress of $\sigma_a^{equ} = 200\ MPa$ in the direction of torsion (Figure 9-b). The combination of the two loads constitutes a sinusoidal biaxial loading and a loading path proportional, which subsequently produces a biaxial pawl, represented by the evolution of the axial stress as a function of the plastic deformation illustrated by hysteresis loops (Figure 9-c). The evolution of the strain angular as a function of the axial strain produced by the same cross loading, shown in Figure 9-d. This experimental database will be used later to perform simulations on 304L steel and to ensure the performance of the model chosen and its ability to describe the nonlinear behavior of the steel studied.
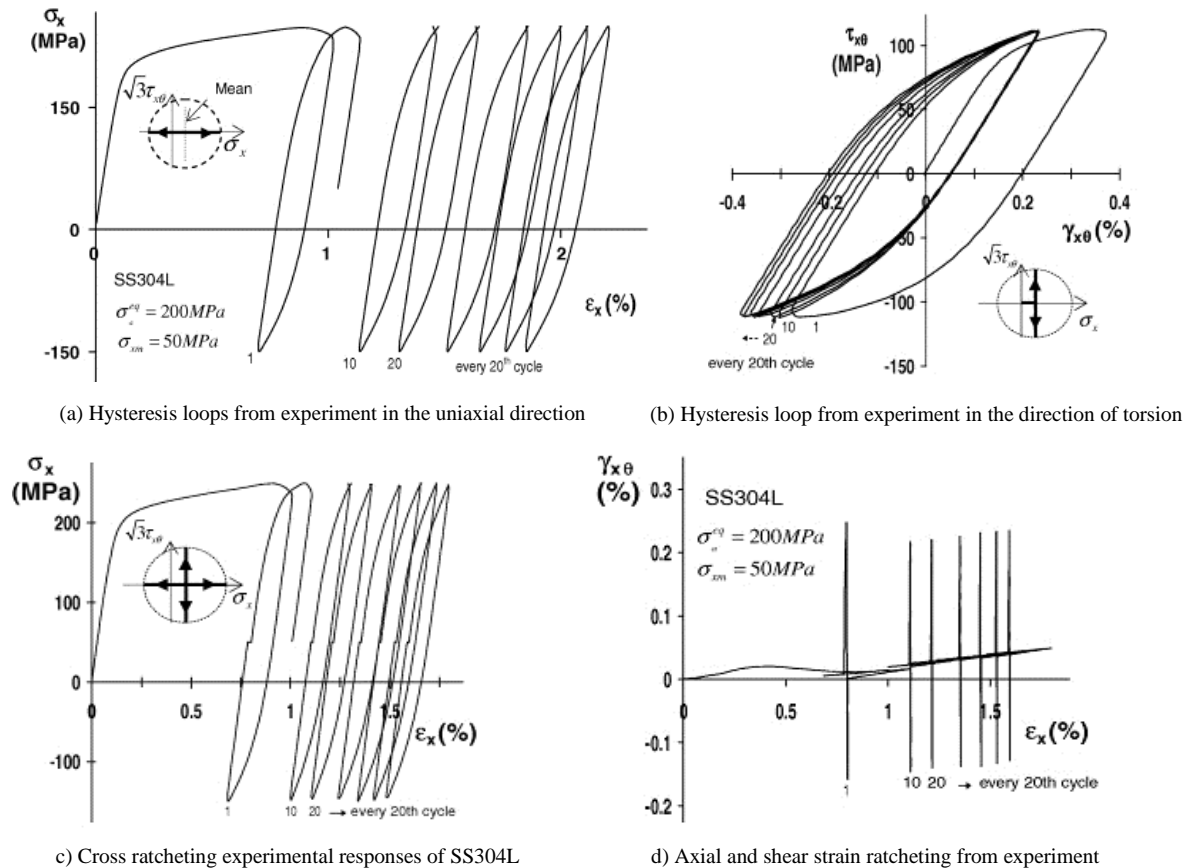

(a) Hysteresis loops from experiment in the uniaxial direction

(b) Hysteresis loop from experiment in the direction of torsion

c) Cross ratcheting experimental responses of SS304L

d) Axial and shear strain ratcheting from experiment

Figure 9. Axial, shear and cross ratcheting experimental responses of SS304L [12]

Johansson et al. (2005) have investigated the prediction of the cyclic behavior of railway points (Figure10-a). The numerical study consists in modeling the plastic deformation at the level of the hinges by a model which is based on the finite elements (Figure 10-b). The numerical results reveal the ratchet phenomenon, controlled in non-zero mean stress, which manifests itself by the evolution of hysteresis loops in the negative direction (Figure 10-c).
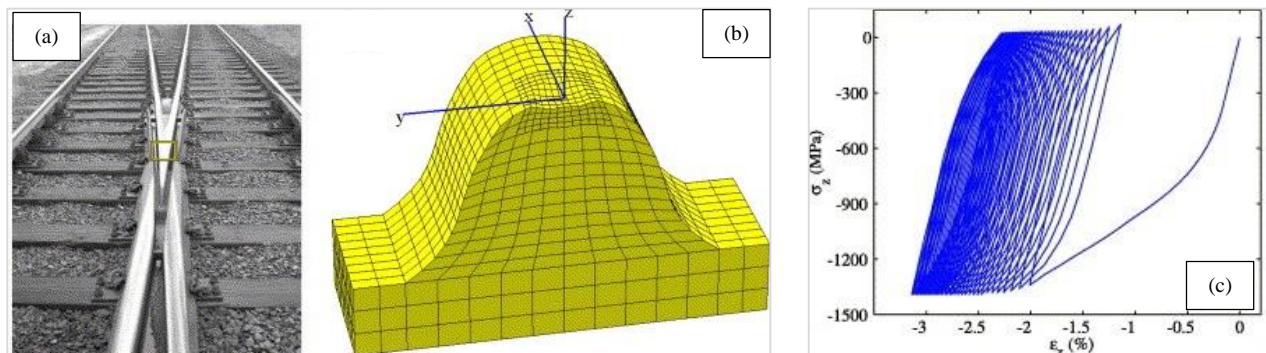

Figure 10. Component of the railway switch subjected to cyclic loading; a) The studied crossing component is marked with a box, b) Deformed geometry of finite element model, c) Uniaxial ratcheting in the Z- direction during 50 cycles [10]

### 5.3.2. Simulation of Biaxial Stress-Controlled Ratcheting Response

In order to understand the ratcheting sensitivity to the mean stress for the 304L steel, some uniaxial cyclic tension simulations were performed with constant stress amplitude. Two strain controlled tests have been performed with the same stresses amplitudes ($\sigma_{a\,=}+125\,MPa$, i): The first history represents a classical uniaxial ratcheting test where 20 cycles of tension-compression is applied about an axial mean stress ($\sigma_{mean=}75MPa$), ii): the second history 20 cycles of tension-compression is applied about negative mean stress ($\sigma_{mean=}-75MPa$), iii): the third story represents 20 cycles of a torsional loading ($\sigma_{x\theta}=\pm150\,MPa$) (see Table 5).

Table 5. Loading conditions (σ: MPa)

Ref.	Loading History	σ_{xmax}	σ_{xmin}	$\sigma_{mean=\frac{\sigma_{max}+\sigma_{min}}{2}}$	$\sigma_a=\frac{\sigma_{max}-\sigma_{min}}{2}$	$R=\frac{\sigma_{min}}{\sigma_{max}}$	$\sigma_{x\theta max}$	$\sigma_{x\theta min}$
Figure 11-a	i	+ 200	- 50	+ 75		- 0.25		
Figure 11-b	ii	+ 50	- 200	- 75	+ 125	4	-	-
Figure 11-c	iii	-	-	-	-	-	+ 150	- 150

In order to test the sensitivity of 304L steel, and to analyze its behavior under repeated multiaxial loading, which was broken down into three simulations. The first two simulations are with loading uni axial asymmetric in mean stress $\sigma_{mean\,=}-75MPa$, developing a positive ratcheting in the direction of traction (Figure11-a) and a mean stress $\sigma_{mean\,=}-75MPa$, offering a negative ratcheting in the direction of compression, Figure 11-b), the third simulation with alternating torsional loading $\sigma_{x\theta}=\pm150MPa$ (Figure 11-c). The combination of the three simulations (Figures 11-a, 11-b, 11-c) shows a multiaxial loading with crossed loading path. There is an accumulation of progressive strain which manifests as a biaxial ratcheting phenomenon diagonally symmetrical with respect to zero stress and strain, and which has evolved in the direction of tension and compression, by hysteresis loops (Figure 11- d). (Figure 11-e) reveals the relationship between the two deformations: angular and axial following multiaxial loading (Figure 11-e).

(a)

(b)

(c)

(d)
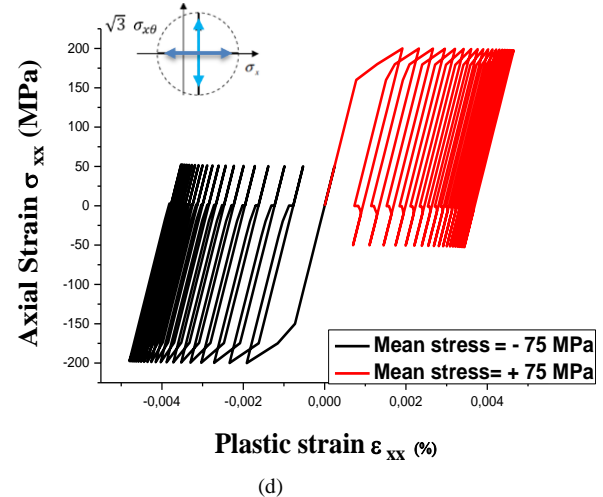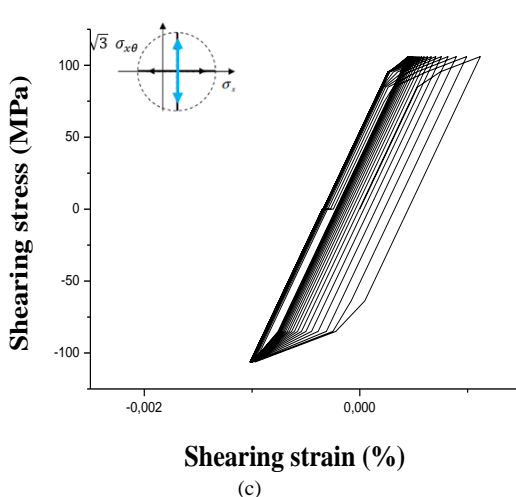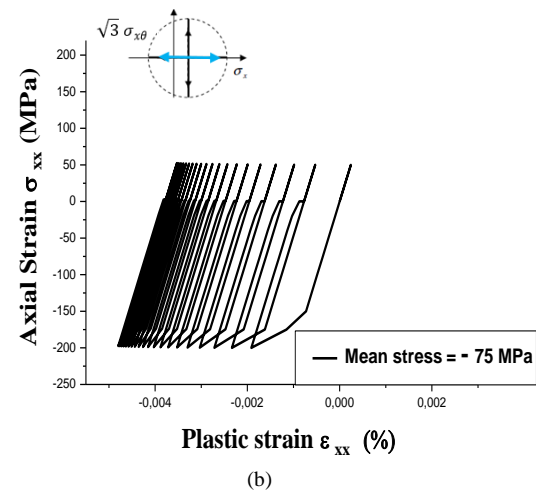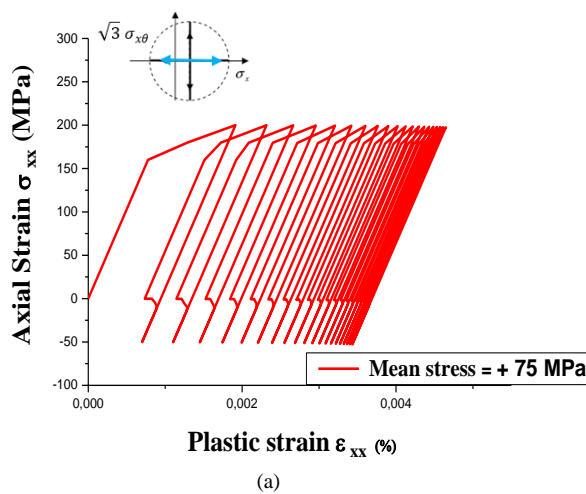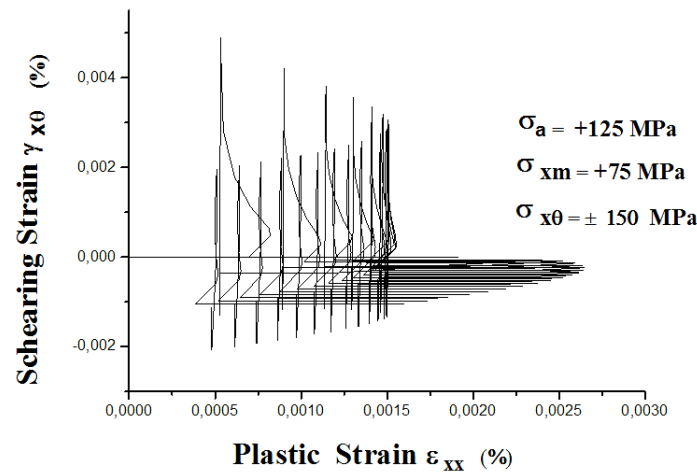
(e)

Figure 11. Ratcheting simulations responses of 304L SS: a) Result of ratcheting for ($\sigma_{mean} = +75MPa$), b) Result of ratcheting for (($\sigma_{mean=} - 75MPa$), c) torsion ratcheting responses, d) manifestation of the ratcheting under the cross path, e) torsion angle as a function of axial strain.

5.4. Comparative Test between 304L and 316L SS

Cross Path Effect in Strain Controlled Tests

The experiment carried out by Taleb and Hauet (2009) [13], consists in carrying out a cyclic test with biaxial loading on steel 304L controlled in strain of 10 cycles $\varepsilon_{xx} = 1$ % applied in the direction of traction-compression, followed by 10 cycles of the alternating equivalent strain of torsion between $\gamma_{x\theta} = \varepsilon_{xx} (\pm\sqrt{3})$. The present simulation was carried out with 50 cycles of traction –compression in the axial direction with imposed strain of $\varepsilon_{xx} = 0.5\%$ followed by 50 cycles of the equivalent strain $\gamma_{x\theta} = 0.86$ % in the direction of torsion. The two loads constitute a cyclic biaxial loading with crossed loading path, carried out on the two steels 304L and 316L (see Table 6).

Table 6. Biaxial sinusoidal loading conditions in imposed strain

Loading path	Ref	Cyclic Test	Tension-compression		Torsion	
			ε_{xx}	ε_{xx}	$\gamma_{x\theta}$	$\gamma_{x\theta}$
	Figure 12	Experience of Taleb and Hauet (2009) [13]	+ 0.1 %	- 0.1%	+ 1.73 %	-1.73 %
	Figure 13	Present Simulation	+ 0.5 %	0.5%	+ 0.86 %	- 0.86 %

Figure 12 represents a cyclic biaxial test carried out on 304L steel performed by Taleb and Hauet (2009) [13], shows the phenomenon of "cross hardening" caused by the additional torsional loading. On the other hand, over hardening is observed on the cyclic curves of 304L and 316L steel in the present study. In addition, the cyclic curve of 304L steel identifies the curve of 316L steel Figure 13.
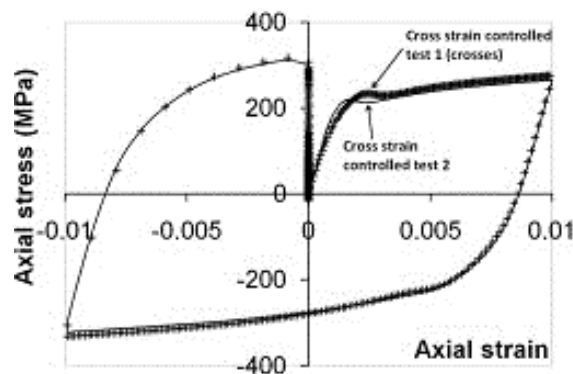

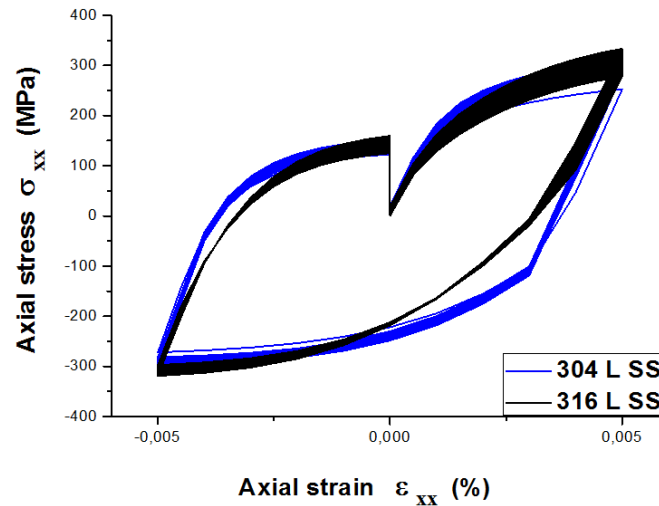**Figure 12. Biaxial test carried out on 304L [13]**

Figure 13. Biaxial simulation test and comparison between 304L and 316L steel

5.4.2. Ratcheting Simulation

The two 304 L and 316L steels will be simulated under bidirectional imposed stress in order to analyze their cyclic behaviors, achieved for a load ratio R = - 0.58 for 100 cycles. The primary loading is applied in the direction of tension–compression around an average stress and an alternating secondary loading applied symmetrically in the direction of torsion. A summary of the simulation conditions is reported in Table 7.

Table 7. Simulation conditions (σ: MPa)

Ref	Loading History	σ_{xmax}	σ_{xmin}	$\sigma_{mean=\frac{\sigma_{max}+\sigma_{min}}{2}}$	$\sigma_{a=\frac{\sigma_{max}-\sigma_{min}}{2}}$	$R=\frac{\sigma_{min}}{\sigma_{max}}$	$\sigma_{x\theta max}$	$\sigma_{x\theta min}$
Figure 14-a	304 L	+ 300	- 175	+ 62.5	+ 137.5	- 0.58	+ 100	100
Figure 14-b	316 L							

Figures 14-a, and 14-b show a biaxial ratcheting of the two 304L and 316L steels, with repeated loading cross loading path. The ratcheting phenomenon is governed by the non-zero mean stress, illustrated by the evolution of the hysteresis loops in the axial direction and represents an excess of progressive strain, which leads to damage. The goal of this simulation is to estimate the optimal biaxial ratcheting, which corresponds to the most relevant progressive strain having a rapid plastic strain intensity, which leads to failure. This simulation was carried out on the two 304L and 316L steels by the superposition of the two ratcheting with the same conditions. It can be seen from Figure 15-a that the optimal biaxial ratcheting corresponds to 316L steel. Note, in the case of using two steels in industry with the same loading conditions, 316L steel will experience rapid failure compared to 304L steel. This estimate has been confirmed by Figure 15-b which represents the evolution of plastic strain as a function of the number of cycles, where we notice that the plastic strain of 316L steel is higher compared to 304L steel.
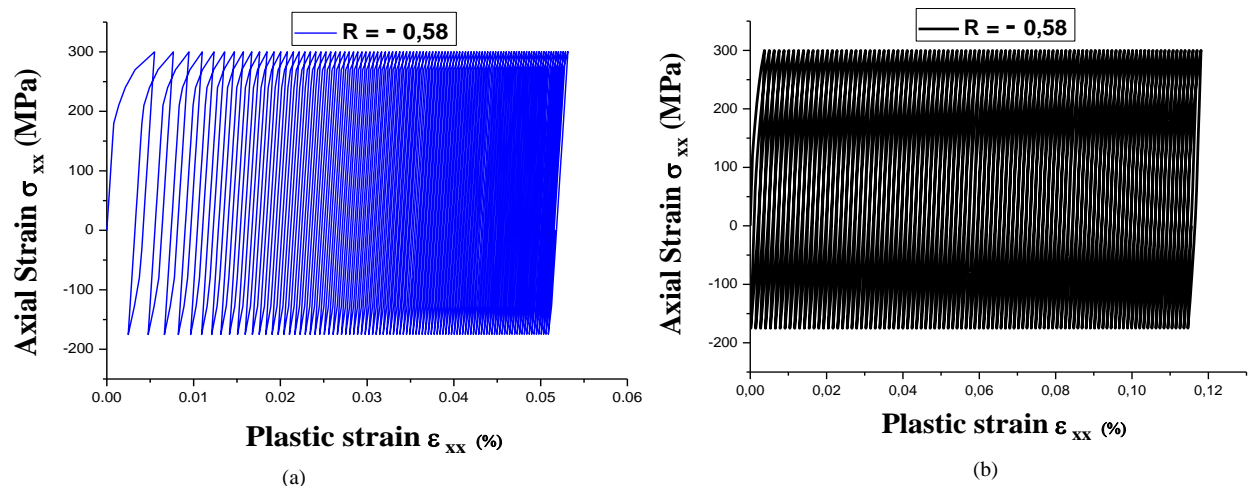

(a)

(b)

Figure 14. Biaxial ratcheting responses: a) results for simulation of 304L SS, b) results for simulation of 316 L SS
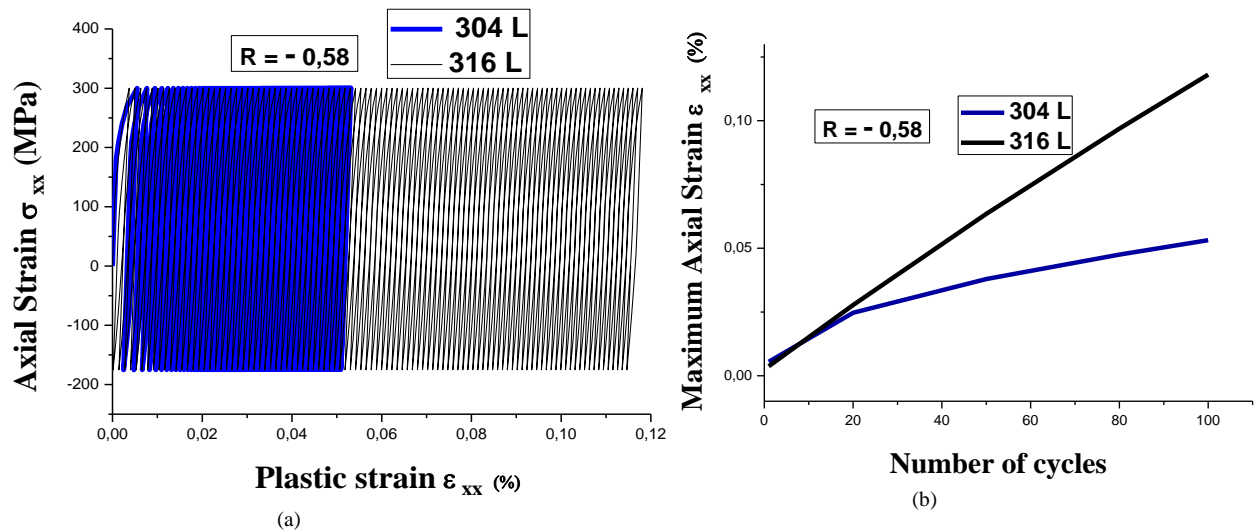
Figure 15. Comparison between progressive deformations : a) superposition of two behaviors of 304L and 316 L steel having the same load ratio R = - 0.58 under biaxial loading, b) Evolution of plastic deformation as a function of the number of cycles of 304 L and 316 L for cross path loading.

6. Conclusion

The aim of this work is thus to make predictions on the behaviour of the two 316L and 304L stainless steels under biaxial stresses. These two alloys are widely used in several fields of industry for their quality and characteristics. The numerical models offer a great capacity to the researchers and specialists in materials and structures for the study and the exploration of different scenarios of loading and multiphysical stresses in order to predict the performances of the alloys and materials distinguished at the shaping of the structures and rooms. The simulated loading consists of two cycles of tensile loading on the uniaxial and torsion on the vertical direction. The results of the simulation obtained on 316L steel under cross loading reveal an optimized ratcheting, which leads to sudden and rapid fracture in two cases: the torsional stress is constant and the axial stress amplitude is low, and the amplitude of the axial stress is constant and the torsional stress is low. The 304L steel investigation illustrates a radially symmetrical rock, for an average stress imposed in two axially opposite directions. Various studies on the behavior of 304L and 316L stainless steel have been carried out by several researchers in recent years. The results presented in this study are discussed with other previous experimental and numerical studies. This comparison shows that the presented results are in good agreement with the results of other previous studies. A comparison was made between the two steels, and it was concluded that the cyclic curve of 304L steel envelops that of 316L steel, for an identical load ratio to imposed strain. On the other hand, the progressive deformation of 316L steel is more accelerated than that of 304L steel in the case where the stress is imposed. As for recommendations, it is suggested to conduct a series of experiments on the two alloys, 304L and 316L, with the same boundary conditions used in this study. This will allow us to build a database that can be used to find out about finite element calculation codes like ZéBulon.

7. Declarations

7.1. Author Contributions

Conceptualization, F.B., K.F.; methodology, T.Z.; software, K.F.; validation, F.B. and T.Z.; formal analysis, T.Z.; investigation, K.F.; resources, K.F.; data curation, F.B.; writing—original draft preparation, F.B.; writing—review and editing, K.F.; visualization, K.F.; supervision, F.B.; project administration, F.B.; funding acquisition, K.F. All authors have read and agreed to the published version of the manuscript.

7.2. Data Availability Statement

The data presented in this study are available in article.

7.3. Funding

The authors received no financial support for the research, authorship, and/or publication of this article.

7.4. Conflicts of Interest

The authors declare no conflict of interest.

8. References

[1] Tong, J., Zhan, Z. L., & Vermeulen, B. (2004). Modelling of cyclic plasticity and viscoplasticity of a nickel-based alloy using Chaboche constitutive equations. International Journal of Fatigue, 26(8), 829–837. doi:10.1016/j.ijfatigue.2004.01.002.

[2] Steglich, D., Pirondi, A., Bonora, N., & Brocks, W. (2005). Micromechanical modelling of cyclic plasticity incorporating damage. International Journal of Solids and Structures, 42(2), 337–351. doi:10.1016/j.ijsolstr.2004.06.041.

[3] Wolff, M., & Taleb, L. (2008). Consistency for two multi-mechanism models in isothermal plasticity. International Journal of Plasticity, 24(11), 2059–2083. doi:10.1016/j.ijplas.2008.03.001.

[4] Böhm, E., Kurek, M., Junak, G., Cieśla, M., & Łagoda, T. (2014). Accumulation of Fatigue Damage Using Memory of the Material. Procedia Materials Science, 3, 2–7. doi:10.1016/j.mspro.2014.06.002.

[5] Lin, Y. C., Chen, X. M., & Chen, G. (2011). Uniaxial ratcheting and low-cycle fatigue failure behaviors of AZ91D magnesium alloy under cyclic tension deformation. Journal of Alloys and Compounds, 509(24), 6838–6843. doi:10.1016/j.jallcom.2011.03.129.

[6] Lu, J., Becker, A., Sun, W., & Tanner, D. (2014). Simulation of Cyclic Plastic Behavior of 304L Steel Using the Crystal Plasticity Finite Element Method. Procedia Materials Science, 3, 135–140. doi:10.1016/j.mspro.2014.06.025.

[7] Mao, J., Engler-Pinto, C. C., Li, T., Hsieh, J., & Su, X. (2015). Effect of Constitutive Model on Thermo-mechanical Fatigue Life Prediction. Procedia Engineering, 133, 655–668. doi:10.1016/j.proeng.2015.12.647.

[8] Kang, G., Gao, Q., Cai, L., & Sun, Y. (2002). Experimental study on uniaxial and non-proportionally multiaxial ratcheting of SS304 stainless steel at room and high temperatures. Nuclear Engineering and Design, 216(1–3), 13–26. doi:10.1016/S0029-5493(02)00062-6.

[9] Kang, G. (2004). A visco-plastic constitutive model for ratcheting of cyclically stable materials and its finite element implementation. Mechanics of Materials, 36(4), 299–312. doi:10.1016/S0167-6636(03)00024-3.

[10] Johansson, G., Ekh, M., & Runesson, K. (2005). Computational modeling of inelastic large ratcheting strains. International Journal of Plasticity, 21(5), 955–980. doi:10.1016/j.ijplas.2004.05.013.

[11] Taleb, L., Cailletaud, G., & Blaj, L. (2006). Numerical simulation of complex ratcheting tests with a multi-mechanism model type. International Journal of Plasticity, 22(4), 724–753. doi:10.1016/j.ijplas.2005.05.003.

[12] Hassan, T., Taleb, L., & Krishna, S. (2008). Influence of non-proportional loading on ratcheting responses and simulations by two recent cyclic plasticity models. International Journal of Plasticity, 24(10), 1863–1889. doi:10.1016/j.ijplas.2008.04.008.

[13] Taleb, L., & Hauet, A. (2009). Multiscale experimental investigations about the cyclic behavior of the 304L SS. International Journal of Plasticity, 25(7), 1359–1385. doi:10.1016/j.ijplas.2008.09.004.

[14] Taleb, L., & Cailletaud, G. (2011). Cyclic accumulation of the inelastic strain in the 304L SS under stress control at room temperature: Ratcheting or creep? International Journal of Plasticity, 27(12), 1936–1958. doi:10.1016/j.ijplas.2011.02.001.

[15] Halama, R., Sedlák, J., & Šofer, M. (2012). Phenomenological Modelling of Cyclic Plasticity. Numerical Modelling. IntechOpen, 329-354. doi:10.5772/35902.

[16] Meggiolaro, M. A., Pinho De Castro, J. T., & Wu, H. (2015). Computationally-efficient non-linear kinematic models to predict multiaxial stress-strain behavior under variable amplitude loading. Procedia Engineering, 101(C), 285–292. doi:10.1016/j.proeng.2015.02.032.

[17] Meggiolaro, M. A., De Castro, J. T. P., Wu, H., & Sanchez, E. C. M. (2016). A general class of non-linear kinematic models to predict mean stress relaxation and multiaxial ratcheting in fatigue problems - Part II: Generalized surface translation rule. International Journal of Fatigue, 82, 167–178. doi:10.1016/j.ijfatigue.2015.08.031.

[18] Boussalih, F., Meziani, S., Fouathia, A., & Fedaoui, K. (2019). Behavior of 304L stainless steel under uniaxial loading and effect of the mean stress on the ratcheting by simulation using chaboche model. UPB Scientific Bulletin, Series D: Mechanical Engineering, 81(2), 179–190.

[19] Belattar, A., & Taleb, L. (2021). Experimental and numerical analyses of the cyclic behavior of austenitic stainless steels after prior inelastic histories. International Journal of Pressure Vessels and Piping, 189, 104256. doi:10.1016/j.ijpvp.2020.104256.

[20] Bocher, L., Delobelle, P., Robinet, P., & Feaugas, X. (2001). Mechanical and microstructural investigations of an austenitic stainless steel under non-proportional loadings in tension-torsion-internal and external pressure. International Journal of Plasticity, 17(11), 1491–1530. doi:10.1016/S0749-6419(01)00013-4.

[21] Chen, X., Jiao, R., & Kim, K. S. (2003). Simulation of ratcheting strain to a high number of cycles under biaxial loading. International Journal of Solids and Structures, 40(26), 7449–7461. doi:10.1016/j.ijsolstr.2003.08.009.

[22] Kulkarni, S. C., Desai, Y. M., Kant, T., Reddy, G. R., Prasad, P., Vaze, K. K., & Gupta, C. (2004). Uniaxial and biaxial ratchetting in piping materials-experiments and analysis. International Journal of Pressure Vessels and Piping, 81(7), 609–617. doi:10.1016/j.ijpvp.2004.04.001.

[23] Kang, G., Li, Y., & Gao, Q. (2005). Non-proportionally multiaxial ratcheting of cyclic hardening materials at elevated temperatures: Experiments and simulations. Mechanics of Materials, 37(11), 1101–1118. doi:10.1016/j.mechmat.2005.01.006.

[24] Poncelet, M., Barbier, G., Raka, B., Courtin, S., Desmorat, R., Le-Roux, J. C., & Vincent, L. (2010). Biaxial high cycle fatigue of a type 304L stainless steel: Cyclic strains and crack initiation detection by digital image correlation. European Journal of Mechanics, A/Solids, 29(5), 810–825. doi:10.1016/j.euromechsol.2010.05.002.

[25] Fremy, F., Pommier, S., Galenne, E., & Courtin, S. (2012). A scaling approach to model history effects in fatigue crack growth under mixed mode I + II + III loading conditions for a 316L stainless steel. International Journal of Fatigue, 42, 207–216. doi:10.1016/j.ijfatigue.2011.10.013.

[26] Rezaiee-Pajand, M., & Sinaie, S. (2013). Calibration of hardening rules for cyclic plasticity. International Journal of Engineering, Transactions A: Basics, 26(4), 351–364. doi:10.5829/idosi.ije.2013.26.04a.04.

[27] Creuziger, A., Hu, L., Gnäupel-Herold, T., & Rollett, A. D. (2014). Crystallographic texture evolution in 1008 steel sheet during multi-axial tensile strain paths. Integrating Materials and Manufacturing Innovation, 3(1), 1–19. doi:10.1186/2193-9772-3-1.

[28] Mazánová, V., Polák, J., Škorík, V., & Kruml, T. (2017). Multiaxial elastoplastic cyclic loading of austenitic 316L steel. Frattura Ed Integrita Strutturale, 11(40), 162–169. doi:10.3221/IGF-ESIS.40.14.

[29] Yaguchi, M., & Takahashi, Y. (2005). Ratchetting of viscoplastic material with cyclic softening, part 2: Application of constitutive models. International Journal of Plasticity, 21(4), 835–860. doi:10.1016/j.ijplas.2004.05.012.

[30] Sai, K., & Cailletaud, G. (2007). Multi-mechanism models for the description of ratcheting: Effect of the scale transition rule and of the coupling between hardening variables. International Journal of Plasticity, 23(9), 1589–1617. doi:10.1016/j.ijplas.2007.01.011.

[31] Chaboche, J. L. (2008). A review of some plasticity and viscoplasticity constitutive theories. International Journal of Plasticity, 24(10), 1642–1693. doi:10.1016/j.ijplas.2008.03.009.

[32] Taheri, S., Hauet, A., Taleb, L., & Kpodekon, C. (2011). Micro-macro investigations about the fatigue behavior of pre-hardened 304L steel. International Journal of Plasticity, 27(12), 1981–2004. doi:10.1016/j.ijplas.2011.06.004.

[33] Budaházy, V., & Dunai, L. (2013). Parameter-refreshed Chaboche model for mild steel cyclic plasticity behaviour. Periodica Polytechnica Civil Engineering (Vol. 57, Issue 2, pp. 139–155). doi:10.3311/PPci.7170.

[34] Saleh, M., Kariem, M. M., Luzin, V., Toppler, K., Li, H., & Ruan, D. (2018). High strain rate deformation of ARMOX 500T and effects on texture development using neutron diffraction techniques and SHPB testing. Materials Science and Engineering A, 709, 30–39. doi:10.1016/j.msea.2017.09.022.

[35] Novak, J. S., Bona, F. De, & Benasciutti, D. (2019). Numerical simulation of cyclic plasticity in mechanical components under low cycle fatigue loading: Accelerated material models. Procedia Structural Integrity, 19, 548–555. doi:10.1016/j.prostr.2019.12.059.

[36] Xie, X. F., Jiang, W., Chen, J., Zhang, X., & Tu, S. T. (2019). Cyclic hardening/softening behavior of 316L stainless steel at elevated temperature including strain-rate and strain-range dependence: Experimental and damage-coupled constitutive modeling. In International Journal of Plasticity (Vol. 114, pp. 196–214). doi:10.1016/j.ijplas.2018.11.001.

[37] Chaboche, J. L. (1989). Constitutive equations for cyclic plasticity and cyclic viscoplasticity. International Journal of Plasticity, 5(3), 247–302. doi:10.1016/0749-6419(89)90015-6.

[38] Djimli, L., Taleb, L., & Meziani, S. (2010). The role of the experimental data base used to identify material parameters in predicting the cyclic plastic response of an austenitic steel. International Journal of Pressure Vessels and Piping, 87(4), 177–186. doi:10.1016/j.ijpvp.2010.02.002.

[39] Besson, J., Leriche, R., Foerch, R., & Cailletaud, G. (1998). Object-oriented programming applied to the finite element method part II. Application to material behaviors. Revue Européenne des Éléments Finis, 7(5), 567-588. doi:10.1080/12506559.1998.10511322.

[40] Roy, S. C., Goyal, S., Sandhya, R., & Ray, S. K. (2013). Analysis of hysteresis loops of 316L (N) stainless steel under low cycle fatigue loading conditions. Procedia engineering, 55, 165-170. doi: 10.1016/j.proeng.2013.03.237.

[41] Moslemi, N., Zardian, M. G., Ayob, A., Redzuan, N., & Rhee, S. (2019). Evaluation of sensitivity and calibration of the chaboche kinematic hardening model parameters for numerical ratcheting simulation. Applied Sciences (Switzerland), 9(12), 2578. doi:10.3390/app9122578.